

Europium doped thiosilicate phosphors of the alkaline earth metals Mg, Ca, Sr and Ba: structure and luminescence

Anthony B. Parmentier, Philippe F. Smet, Dirk Poelman

LumiLab, Department of Solid State Sciences, Ghent University, Ghent, Belgium

Abstract

Divalent europium is notorious for the tunability of its emission, depending on the host material in which it is used as a dopant. In europium-doped alkaline earth thiosilicates, two distinct emission bands can be observed for the alkaline earth metals Mg, Ca and Sr while only a single band is found for barium thiosilicate. In this work, we first complete the data with europium-doped magnesiumthiosilicate. Then, the solid solution of calcium and magnesium thiosilicate is presented. To conclude, the presence of multiple emission peaks in some compounds is explained on a structural basis, by analysing the possibilities for preferential orientation of the europium d-orbitals.

Keywords: Eu²⁺, thiosilicates, phosphor, Mg₂SiS₄, Ca₂SiS₄, Sr₂SiS₄, Ba₂SiS₄

1. Introduction

The luminescence of Eu²⁺ in alkaline earth thiosilicates with composition M₂SiS₄ was first reported by Avella [1] (cathodoluminescence; M = Mg,

Email address: philippe.smet@ugent.be (Philippe F. Smet)

4 Ca, Sr and Ba) and Olivier-Fourcade [2] (cathodo- and photoluminescence;
 5 $M = \text{Sr, Ba}$). They reported one single emission peak for each alkaline earth.
 6 Avella attributed the additional peaks he observed in $\text{Mg}_2\text{SiS}_4\text{:Eu}^{2+}$ and
 7 $\text{Ca}_2\text{SiS}_4\text{:Eu}^{2+}$ to (trace amounts of) the binary sulfides MgS and CaS . Smet
 8 rebuked this claim for $M = \text{Ca}$, and showed that both Eu^{2+} -emission peaks
 9 are due to the Ca_2SiS_4 -host [3]. The short-wavelength emission (565 nm)
 10 dominates at low Eu^{2+} -concentrations ($<1\%$), while the long-wavelength
 11 peak (660 nm) does at larger concentrations. For $\text{Ba}_2\text{SiS}_4\text{:Eu}^{2+}$, the sin-
 12 gle emission band (500 nm) was confirmed [4]. Two distinct emission bands
 13 can be observed for $\text{Sr}_2\text{SiS}_4\text{:Eu}^{2+}$ [5], a long wavelength peak (550 nm) and a
 14 short wavelength peak (490 nm). At room temperature, the latter is visible
 15 only for certain excitation wavelengths and for low dopant concentrations.
 16 At low temperature however, it is clearly resolved.

17 The scope of this work is two-fold: First, new results on the structure and
 18 photoluminescence of thiosilicate phosphors are presented. In particular, we
 19 report the photoluminescent and structural characteristics of $\text{Mg}_2\text{SiS}_4\text{:Eu}^{2+}$
 20 and of the solid solution $\text{Ca}_{2x}\text{Mg}_{2(1-x)}\text{SiS}_4\text{:Eu}^{2+}$ with $0 \leq x \leq 1$. Then, based
 21 on both the previously published data and on the new results, a structural
 22 explanation for both the double emission bands in the thiosilicates of Mg,
 23 Ca, Sr and the single band in Ba_2SiS_4 , is proposed. We can use the concept
 24 of preferential orientation of the europium 5d-orbitals to explain why there
 25 are two bands for the former, but only one for the latter.

26 An additional long wavelength band, next to the normal Eu^{2+} emission
 27 band, that cannot be caused by the coordination of the Eu^{2+} -sites with the
 28 anions, occurs in several other compounds [6, 7, 8, 9]. Poort et al. relate

29 this to a preferential orientation of one or more 5d-orbitals of Eu^{2+} , caused
 30 by the alkaline earth cations that surround the Eu^{2+} -ion. The stronger the
 31 preferential orientation, the lower the energy of the orbital becomes, and thus
 32 the longer the wavelength of the emission. They state that this preferential
 33 orientation occurs within (different types of) rows or chains. An important
 34 condition is that the interatomic distance in the row should be smaller than
 35 the distance to the next row of alkaline earth metals.

36 **2. Experimental**

37 The preparation of M_2SiS_4 (with $\text{M} = \text{Mg}, \text{Ca}, \text{Sr}, \text{Ba}$) from MS , Si and
 38 H_2S was described elsewhere [3, 4, 5]. The MgS used was 99.5 % grade (GFS
 39 Chemicals). A 5 % excess of Si was added as powder to the initial mixture,
 40 to compensate for silicon losses during sintering. Sintering temperature was
 41 825°C . Eu^{2+} -concentration in M_2SiS_4 was 2% in all samples. Mg_2SiS_4 -
 42 samples with Eu^{2+} -concentration of 0.2%, 0.5% and 1% were also prepared.

43 A Bruker D5000 diffractometer in $\theta-2\theta$ geometry, was used to record
 44 XRD patterns from $\text{Cu K}\alpha$ radiation.

45 Lattice constants and atomic positions in the unit cell were obtained
 46 using the Fullprof software package [15]. The initial parameters used for the
 47 refinement stem from various sources, an overview is given in Table 1. When
 48 data are not available, analogous structures are used as a starting point.
 49 (E.g. atomic positions of Mg_2SiS_4 were based on these of Mg_2GeS_4 .)

50 Photoluminescence emission and excitation spectra were recorded using
 51 a FS920 fluorescence spectrometer (Edinburgh Instruments). Variation of
 52 the measurement temperature (70 K–450 K) is obtained by an Optistat CF

M ²⁺	Lattice parameters	Atomic positions	Space group
Mg	Mg ₂ SiS ₄ [10]	Mg ₂ GeS ₄ [11]	62 (<i>Pnma</i>)
Ca	Ca ₂ SiS ₄ [3]	Ca ₂ GeS ₄ [12]	62 (<i>Pnma</i>)
Sr	Sr ₂ SiS ₄ [5]	Eu ₂ SiS ₄ [13]	11 (<i>P2</i> ₁ /m)
Ba	Ba ₂ SiS ₄ [14]		62 (<i>Pnma</i>)

Table 1: Overview of data used for structural analysis.

helium cryostat (Oxford Instruments) placed inside the spectrometer.

3. Results and discussion

3.1. *Mg₂SiS₄·Eu²⁺*

As MgS is very hygroscopic (exposing it to the ambient air for one day, completely decomposes the compound), the preparation of Mg₂SiS₄ (as well as the mixtures with MgS as starting material) proved to be more cumbersome than that of the thiosilicates of Ca, Sr and Ba. All synthesized powders contain small amounts of impurities of e.g. MgS and MgO, as indicated in the XRD-data shown in Figure 1. The XRD patterns of Mg₂SiS₄ fit well to an orthorhombic structure (space group *Pnma*, n°62) with lattice parameters $a = 12.67 \text{ \AA}$; $b = 7.41 \text{ \AA}$; $c = 5.91 \text{ \AA}$. This result is in agreement with literature [10]. The main peaks of a simulated XRD pattern (dots) with these parameters are shown for comparison in Figure 1.

When compared with a typical XRD spectrum of the other thiosilicates (not shown), the background signal is larger in samples where Mg is present, indicating a larger amount of amorphous material. The lower quality of the

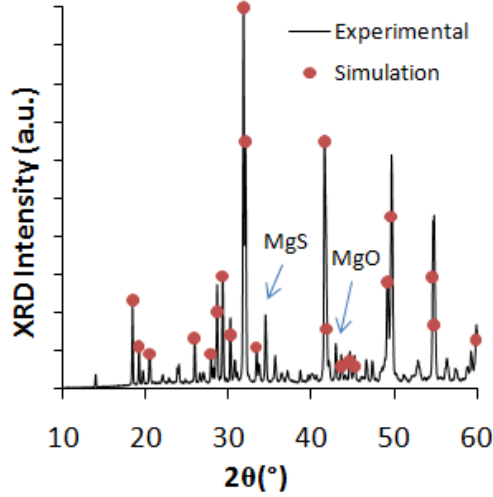


Figure 1: Measured XRD pattern (solid line) of $\text{Mg}_2\text{SiS}_4:2\%\text{Eu}^{2+}$ compared with XRD-simulation (dots). MgS and MgO impurities are also indicated.

69 powders that contain Mg, as compared with the other thiosilicates, can be
 70 attributed to the higher hygroscopicity of MgS.

71 The PL spectrum of $\text{Mg}_2\text{SiS}_4:0.2\%\text{Eu}^{2+}$ in Figure 2 consists of two
 72 emission bands peaking at 560 ± 5 nm and 655 ± 5 nm. Their relative inten-
 73 sity depends on the excitation wavelength and on the Eu^{2+} -concentration.
 74 There is a considerable overlap between the excitation spectrum of the long-
 75 wavelength band and the emission of the short-wavelength band. The inten-
 76 sity of the emission is low in comparison with the ones of e.g. $\text{Ca}_2\text{SiS}_4:\text{Eu}^{2+}$
 77 and $\text{Sr}_2\text{SiS}_4:\text{Eu}^{2+}$ with comparable concentrations. No significant MgS: Eu^{2+} -
 78 emission (590 nm) can be identified in the spectra. Nevertheless, considering
 79 the presence of several undesired phases in small quantities, it cannot be ex-
 80 cluded that the emission spectrum contains a small contribution originating
 81 from these phases.

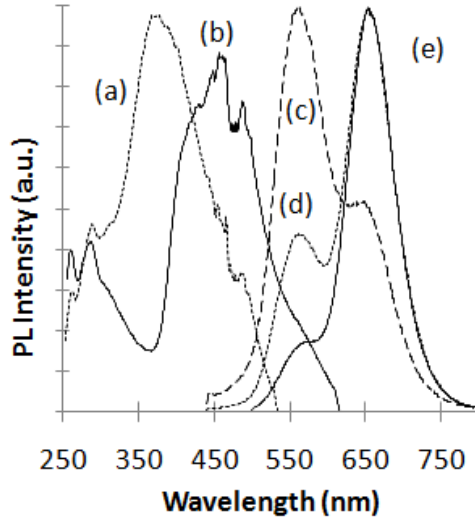


Figure 2: PL Spectrum of $\text{Mg}_2\text{SiS}_4:0.2\% \text{Eu}^{2+}$, (a),(b) Excitation spectra monitored at 560 nm and 655 nm; (c),(d),(e) Emission spectra, excited at 365 nm, 400 nm and 450 nm

82 The behaviour of the emission as a function of temperature is represented
83 in Figure 3. The short wavelength peak is rapidly quenched, dropping to
84 half its low-temperature intensity around 265 K. The quenching behaviour
85 of the long wavelength band is clearly different. At temperatures of >440 K,
86 the intensity of the band has not yet dropped to half its low-temperature
87 value. Determining a general thermal quenching temperature as the temper-
88 ature at which the integrated emission intensity has dropped to half its low-
89 temperature value, we get 400 ± 10 K, inbetween the values for $\text{Ca}_2\text{SiS}_4:\text{Eu}^{2+}$
90 (460 K) and $\text{Sr}_2\text{SiS}_4:\text{Eu}^{2+}$ (380 K).

91 As the thermal quenching temperature of $\text{Mg}_2\text{SiS}_4:\text{Eu}^{2+}$ is well above
92 room temperature, the low intensity of the emission cannot be attributed to
93 it being thermally quenched. The body colour of the thiosilicates doped with
94 europium is usually very distinct, but the body colour of the doped Mg_2SiS_4 -

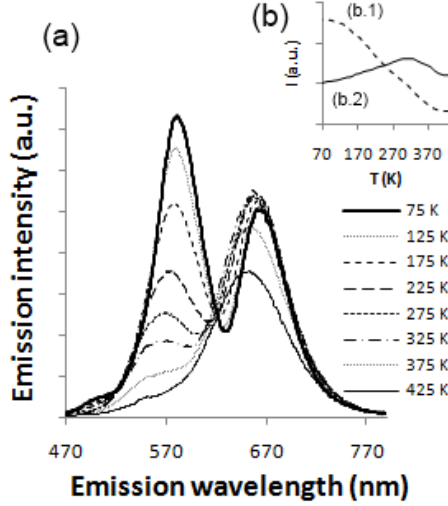


Figure 3: (a) PL Emission of $\text{Mg}_2\text{SiS}_4:0.5\% \text{Eu}^{2+}$, excited with 400 nm light, monitored from 70 K up to 440 K (b) PL intensity as a function of temperature, (b.1) for the short-wavelength peak and (b.2) for the long-wavelength peak

95 samples is consistently whitish. This suggests that the Eu^{2+} -ion is poorly
 96 incorporated in this host, which does not seem implausible, considering the
 97 ion size difference between Mg^{2+} and Eu^{2+}

98 3.2. $(\text{Ca}, \text{Mg})_2\text{SiS}_4:\text{Eu}^{2+}$

99 As both the thiosilicate of Ca and of Mg have orthorhombic $Pnma$ struc-
 100 ture, it is expected that the solid solution of $(\text{Ca}, \text{Mg})_2\text{SiS}_4$ has the same
 101 space group. The change in XRD-pattern as a function of composition is
 102 represented in both Figure 4 and Table 2. It can be seen from Table 2 that
 103 the lattice expands upon substituting Mg^{2+} by the larger Ca^{2+} . The data
 104 also indicate that up to 75 % of Mg^{2+} can replace the Ca^{2+} -ions in Mg_2SiS_4 ,
 105 with only a minor reduction in the dimensions of the unit cell.

106 The change of the photoluminescent emission as a function of compo-

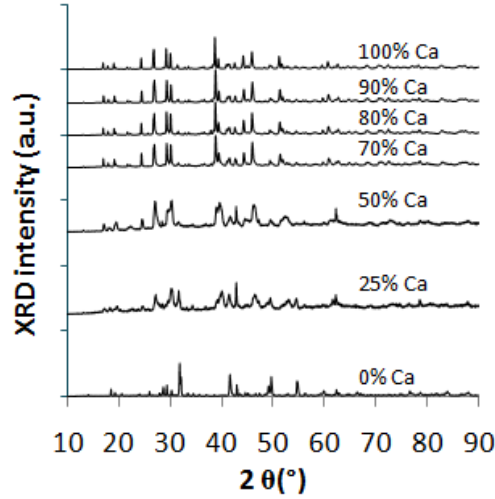


Figure 4: Measured XRD-patterns of the solid solution $(\text{Ca}_x\text{Mg}_{1-x})_2\text{SiS}_4$ for $x=0..1$. On top is the XRD-pattern of Ca_2SiS_4 , and at the bottom that of Mg_2SiS_4 . In between, some intermediate compositions are shown

107 sition can also be found in Table 2. As an example, the PL spectrum of
 108 $(\text{Ca}_{0.5}\text{Mg}_{0.5})_2\text{SiS}_4:2\%\text{Eu}^{2+}$ with two gaussian bands (fitting done on energy
 109 scale) is represented in Figure 5. Looking at the short wavelength peak, one
 110 notices an increase in emission wavelength, for compositions with up to 75 %
 111 of Mg^{2+} . For the fully substituted Mg_2SiS_4 , the peak shifts back to shorter
 112 wavelength.

113 Similar to the case in MgS , the large Eu^{2+} -ion locally distorts the host
 114 lattice [16], reducing the red-shift caused by the crystal field, reducing the
 115 anticipated red-shift caused by the crystal field. ??

116 3.3. $\text{M}_2\text{SiS}_4:\text{Eu}^{2+}$ overview ($M = \text{Mg}, \text{Ca}, \text{Sr}, \text{Ba}$)

117 The thiosilicates of Mg, Ca and Sr have 2 separate emission bands.
 118 Ba_2SiS_4 has a single emission band. For all four cations, the sulfur-coordination

% Ca	a (Å)	b (Å)	c (Å)	λ_1 (nm)	λ_2 (nm)
100	13.54	8.22	6.22	565	664
90	13.52	8.18	6.20	565	663
80	13.50	8.17	6.19	566	665
70	13.49	8.15	6.18	567	659
50	13.45	8.06	6.08	581	669
25	13.41	7.81	6.05	579	643
0	12.67	7.41	5.91	560	655

Table 2: The refined lattice parameters and the emission peaks of $(\text{Ca,Mg})_2\text{SiS}_4:2\% \text{Eu}^{2+}$ as a function of composition

119 is very similar for both alkaline earth sites. (To illustrate this, the minimum
 120 and maximum distances from the M^{2+} -ions to the nearest neighbours are
 121 given in Table 3.) In fact, in Ba_2SiS_4 , the SiS_4^{4-} tetrahedra show the high-
 122 est distortion, and the distances from Ba to S differ more than they do for
 123 the other thiosilicates. A difference in sulfur coordination is thus clearly not
 124 the cause of the two emission bands, as this would have the opposite effect.
 125 Also, the distance from each alkaline earth to the nearest silicon is about the
 126 same for both sites. The difference must therefore be due to the coordination
 127 of an alkaline earth site with the next one(s). Therefore, in the next para-
 128 graphs, we analyse the possibilities for preferential orientation of the divalent
 129 europium in these hosts.

130 The thiosilicates of Mg and Ca can be treated together, because they have
 131 a very similar structure. The lattice of both is orthorhombic, Mg (Ca) atoms
 132 are arranged in rows, at a distance of 3.71 (4.11) Å, being half the lattice

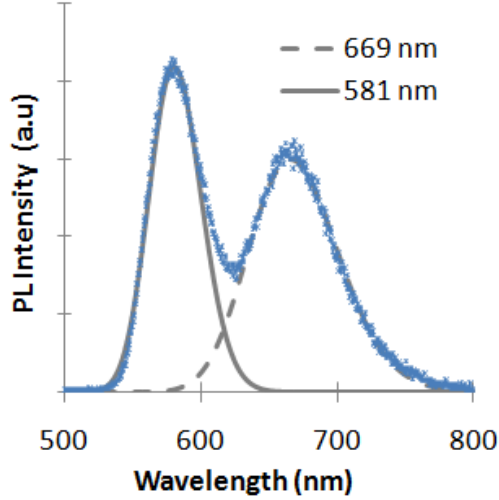


Figure 5: The emission spectrum of CaMgSi_4 , together with the two best fitting gaussian curves. Excitation wavelength is 400 nm.

constant along the b-axis. The distance to the next row is 5.91 (6.22) Å (the
lattice constant along the c-axis), clearly larger than the distance within the
row. Therefore, d-orbitals of Eu^{2+} will orient preferentially along the b-axis,
thus lowering their energy and forming the long wavelength band visible
in the emission spectra of Mg_2SiS_4 (Ca_2SiS_4). The Eu^{2+} d-orbitals on this
crystallographic site that are not oriented preferentially, give rise to emission
at shorter wavelength, as do the europium ions that occupy the second Mg
(Ca) site, which is not a part of any row or chain. Therefore, no possibility
for preferential orientation exists for the atoms occupying this site.

For the thiosilicate of Sr, the situation is different. The crystal structure is
monoclinic, and the Sr-atoms do not line up in a perfect linear row. However,
the atoms of both sites alternate at distances of 4.12 Å and 4.25 Å, the angles
between the lines that connect the Sr-atoms being around 168°. This can

M^{2+}	M-S		distance	distance
	min.	max	in row(\AA)	to next row (\AA)
Mg	2.5	2.6	3.71	5.91
Ca	2.7	2.9	4.11	6.22
Sr	2.9	3.1	4.11/4.25	5.26
Ba	3.1	3.4	no rows	

Table 3: Key distances in the alkaline earth thiosilicate lattices.

clearly give rise to a preferential direction, along which d-orbitals of the europium-ion can orient.

Finally, in Ba_2SiS_4 no rows whatsoever can be found. Therefore, in this host there is no possibility for the Eu^{2+} -ion to orient preferentially. The emission spectrum is thus a single emission peak.

The emission spectra of all alkaline earth metals, measured at low temperature (70 K) and excited at 400 nm are shown in Figure 6. In thiosilicates, emission wavelength range from 490 nm to 660 nm (Figure 6) can be obtained by doping with Eu^{2+} and variation of the composition of the host.

4. Conclusion

The emission spectra of the solid solution $(\text{Ca},\text{Mg})_2\text{SiS}_4$ do not vary very much with composition. The replacement of part of the Ca^{2+} -ions in Ca_2SiS_4 by Mg^{2+} -ions proves not beneficial for practical application, since the preparation of the material is complicated by the addition of by the unstable MgS . Furthermore, several phosphor characteristics (emission intensity, thermal quenching temperature, ...) deteriorate on substitution of Ca by Mg.

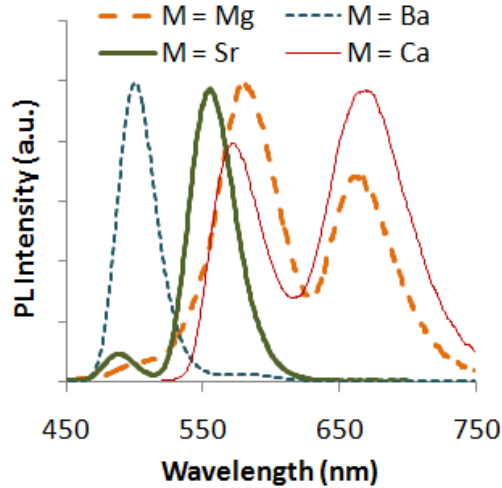


Figure 6: Normalised emission spectra of the europium-doped alkaline earth thiosilicates. The gap between 550 nm and 660 nm can be filled with the solid solution $(\text{Ca,Sr})_2\text{SiS}_4$.

162 The occurrence of two emission bands in Mg, Ca and Sr thiosilicate and
 163 the presence of only one band in Ba_2SiS_4 is explained qualitatively in terms of
 164 preferential orientation of the d-orbitals of Eu^{2+} . The difference is not due to
 165 difference in interaction with the S atoms or with the SiS_4^{4-} -tetrahedra, but
 166 it is due to a different interaction of the Eu^{2+} -ion with the nearest alkaline
 167 earth metals of the host.

- 168 [1] F. J. Avella, J. Electrochem. Soc. 118 (1971) 1862-1863.
- 169 [2] J. Olivier-Fourcade, M. Ribes, E. Philippot, P. Merle, M. Maurin, Mater.
 170 Res. Bull. 10 (1975) 975-982.
- 171 [3] P. F. Smet, N. Avci, B. Loos, J. E. Van Haecke, D. Poelman, J. Phys.:
 172 Condens. Matter 19 (2007) 246223.

- 173 [4] P.F. Smet., K. Korthout, J.E. Van Haecke, D. Poelman Mater. Sci. Eng.
174 B 146 (2008) 264268
- 175 [5] A. B. Parmentier, P. F Smet, F. Bertram, J. Christen, D. Poelman, J.
176 Phys. D: Appl. Phys. 43 (2010) 085401.
- 177 [6] S. H. M. Poort, W. P. Blokpoel, G. Blasse, Chem. Mater. 7 (1995)
178 1547-1551.
- 179 [7] S.H.M. Poort, H.M. Reijnhoudt, H.OT. van der Kuip, G. Blasse, J.
180 Alloys Compd. 241 (1996) 75-81.
- 181 [8] S. H. M. Poort, J. W. H. van Krevel, R. Stomphorst, A. P. Vinck, G.
182 Blasse, J. Solid State Chem. 122 (1996) 432-435.
- 183 [9] S.H.M. Poort, W. Janssen, G. Blasse, J. Alloys Compd. 260 (1997) 93-
184 97.
- 185 [10] H. Vincent, E.F.Bertaut, Acta Cryst. B 32 (1976) 1749.
- 186 [11] H. Vincent, G. Perrault, Bull. Soc. Fr. Minéral. Cristallogr. 94 (1971)
187 551-555.
- 188 [12] M. Ribes, E. Philippot, M. Maurin, C. R. Acad. Sc. Paris C 270 (1970)
189 716.
- 190 [13] D. Johrendt, R. Pocha, Acta Cryst. E 57 (2001) i57-i59.
- 191 [14] R. Dumail, M. Ribes, E. Philippot, C. R. Acad. Sc. Paris C 272 (1971)
192 303.
- 193 [15] J. Rodríguez-Carvajal, Physica B 192 (1993) 55-69.

- 194 [16] P. F. Smet, J. E. Van Haecke, F. Loncke, H. Vrielinck, F. Callens, D.
195 Poelman, Phys. Rev. B: Condens. Matter 74 (2006) 035207.
- 196 [17] H. Kasano, K. Megumi, H. Yamamoto, J. Electrochem. Soc. 131 (1984)
197 1953-1960